Received: 22 February 2019 | Revised: 21 August 2019 | Accepted: 9 September 2019

DOI: 10.1002/ppp3.10080

RESEARCH ARTICLE

Plants People Planet PPP Open Access

Hyperspectral assessment of plant responses to multi-stress environments: Prospects for managing protected agrosystems

Lorenzo Cotrozzi | **John J. Couture**

Departments of Entomology and Forestry and Natural Resources and Purdue Center for Plant Biology, Purdue University, West Lafayette, IN, USA

Correspondence
John J. Couture, Departments of Entomology and Forestry and Natural Resources and Purdue Center for Plant Biology, Purdue University, 901 W State Street, West Lafayette, IN 47907, USA.
Email: couture@purdue.edu

Present address
Lorenzo Cotrozzi, Department of Agriculture, Food and Environment, University of Pisa, Via del Borghetto, 80, 56124, Pisa, Italy

Funding information
USDA NIFA, Grant/Award Number: IND011490

Societal Impact Statement

Advancements in our ability to rapidly detect plant responses to stress are necessary to improve crop management practices and meet the global challenge of food security. Using optical approaches to detect plant stress before symptoms become apparent has great potential, but these approaches lack testing in multiple-stress environments and fail to fully exploit the data collected. Using hyperspectral data from lettuce, we show that optical measurements can provide growers with important stress-related information to inform crop management practices. We suggest that integrating this technology into protected agrosystems, such as greenhouses, could greatly improve crop quality and yield.

Summary

- Tools to detect and predict stress pre-visually are essential to optimally manage agrosystems. Here, we investigated the capability of reflectance spectroscopy to characterize responses of asymptomatic crop leaves under multi-stress conditions.
- Full range (350–2,500 nm) reflectance measurements and traditional plant stress responses were collected on lettuce leaves under the combination of different supplemental light types and intensities, fertilization and salinity. Partial least-squares discriminate analysis and regression modeling and spectral indices were employed to characterize plant responses to multiple stress conditions, both alone and in combination.
- Spectral profiles (400–800 nm + 1,900–2,200 nm) of individuals grown under variable environments were statistically different ($p < .05$) for multiple combinations. Partial least-squares discriminate analysis accurately classified the different single stressors well (accuracy: 0.76–0.91), but generated moderate accuracies (0.63–0.65) for two-stress combinations, and low accuracy (0.33) for higher order stress combinations. Osmotic potential, and chlorophyll and phenol concentrations were well predicted by spectral data (validation R^2: 0.70–0.84). Higher lettuce yield and quality was found under sodium light at high intensity (850 µmol m^{-2} s^{-1} photosynthetic active radiation), with high fertilization (150 ppm N) and no salinity.

- Our findings highlight the utility and limitations of vegetation spectroscopy in a protected agrosystem. We suggest that integration of vegetation spectroscopy into intelligent and automated greenhouses and other protected systems could enhance management efficiency, as well as crop quality and yield.

KEYWORDS

crop management, hyperspectral phenotyping, *Lactuca sativa*, partial least squares discriminant analysis, partial least squares regression, vegetation indices

1 | INTRODUCTION

Global demand for agricultural crops is increasing, and may continue to do so for decades, propelled by a projected 2.3 billion person increase in global population and a continued rise in per capita incomes by 2050 (Godfray et al., 2010). A major goal of plant breeding is increasing crop production and nutritional content, with the latter being especially important for species that will be cultivated in low-income areas (Gascuel, Diretto, Monforte, Fortes, & Granell, 2017). In efforts to increase growing season length to enhance production, there has been an increase in protected growing environments, such as greenhouses, high tunnels, and chamber-based production systems. In these systems, crop productivity and quality are affected by different environmental factors than crops from field production systems, such as light intensity and salinity, as well as over fertilization, which can exacerbate other environmental issues affecting production (Cotrozzi & Landi, 2018; DaMatta, Grandis, Arenque, & Buckeridge, 2010; Godfray et al., 2010; Mickelbart, Hasegawa, & Bailey-Serres, 2015).

Exposure to non-optimal conditions for a short period of time usually increases plant antioxidant metabolism to counteract oxidative stress, and as a consequence improves nutritional quality (Pérez-López, Miranda-Apodaca, Lacuestra, Mena-Petite, & Munõz-Rueda, 2015). This outcome may represent an optimal choice for growers, enhancing plant nutritional quality, especially under controlled conditions. Thus, early diagnosis (e.g., before visible symptoms) of plant responses to environmental variation is important to maximize plant nutritional status yet avoid negative consequences for biomass and yield production. It is also important to assess the effects of combined environmental factors, especially when the plant response to the collective effect is dissimilar to the plant response to singular environmental factors (Pandey, Irulappan, Bagavathiannan, & Senthil-Kumar, 2017; Pellegrini et al., 2019). Advancements in phenotyping techniques that can detect and monitor plant responses to environmental variation before the onset of visual symptoms can concomitantly increase crop yield and quality, and optimize management and input efforts.

The need for rapid and non-destructive assessments of plant status, along with the potential to simultaneously assess multiple traits on a large number of individual plants over multiple time periods, has led to the development of new, and the re-evaluation of existing, sensor technologies from various scientific domains (Li, Zhang, & Huang, 2014). One such emerging sensor technology is vegetation spectroscopy. This emergence is a result of improvements in the sensitivity and portability of spectrometers, as well as increases in computational capabilities and advancement of chemometric modeling methods. These developments have enabled the estimation of a wide variety of plant chemical properties and physiological processes based on the foliar optical properties of living tissue. The estimation of these traits from leaf reflectance relies on variations in absorption of molecular organic bonds, primarily C-H, N-H, and O-H bonds, resulting in vibrational excitation at specific wavelengths of the electromagnetic spectrum. The exploitation of the relationships of light with organic bonds provides the ability of vegetation spectroscopy to characterize plant chemical and physiological status.

In the visible region (VIS; 400–700 nm), plant pigments absorb most of the incident light, while larger molecules, such as carbohydrates, proteins and water have characteristic absorption features in the near-infrared (NIR; 700–1,100 nm) and short-wave infrared (1,100–2,400 nm) spectral regions (Cotrozzi, Townsend, Pellegrini, Nali, & Couture, 2018; Deacon, Grossman, Schweiger, Armour, & Cavender-Bares, 2017). Simple spectral reflectance vegetation indices based on the ratio of reflected light at different wavelengths have been developed to predict foliar traits concerning the structure of vegetation, and can correlate with biochemistry and plant physiology or stress conditions (e.g., photochemical reflectance index [PRI]; Gamon, Serrano, & Surfus, 1997; normalized difference water index [NDWI]; Gao, 1996). A more recent and expanding approach models plant traits directly as a function of the spectral profile using multivariate methods such as partial least squares regression (PLSR; Wold, Sjöström, & Eriksson, 2001). The model calibration is accomplished by pairing leaf spectra, collected in a consistent manner using a uniform and stable illumination source, with independent and reliable measurements. These models are validated using independent samples, and can then be used to predict the variable of interest in unknown samples on the basis of their spectral reflectance alone (Couture & Lindroth, 2012).

To date, a number of foliar morphological, physiological, and biochemical traits have been successfully quantified from spectra using this approach (Asner & Martin, 2008; Asner et al., 2011; Cotrozzi et al., 2017; Couture, Serbin, & Townsend, 2013; Couture et al., 2016; Petisco et al., 2006; Serbin et al., 2015). However, while phenotypic information can be informative in identifying and managing crop productivity and quality, individual traits are rarely sufficient for crop management. Spectra themselves are a phenotypic expression of the aggregate signals of chemical, morphological and physiological properties of leaves under specific environmental conditions and management practices (Cavender-Bares et al., 2016). Consequently, spectral characteristics of plants measured across a wide range of wavelengths could potentially provide important information for crop selection and management (i.e., hyperspectral phenotyping). The use of hyperspectral reflectance as a powerful phenotyping tool in agricultural research is promising (Couture et al., 2018; Li et al., 2014; Serbin et al., 2015; Silvia-Perez et al., 2017; Yendrek et al., 2017), but questions remain regarding limitations of the technique, such as its capability in more complex, multifactorial experiments.

Lettuce (*Lactuca sativa* L.) is a major greenhouse-grown crop that is consumed worldwide and ranks as one of the top ten most valuable crops in the United States with an annual value of over $2.4 billion (Reyes-Cin-Wo et al., 2017). This popular green vegetable contributes fiber, vitamins A, C, and E, carotenoids, calcium, potassium, magnesium and phenolic acids to the diet of the consumer (Nicolle et al., 2004). Lettuce is considered a model crop for studying the impact of light quality on plant responses (Saito, Shimizu, Nakashima, Miyasaka, & Ohdoi, 2010; Samoulienė, Sirtautas, Brazaitytė, & Duchovskis, 2012; Wang, Lu, Tong, & Yang, 2016) and is also considered to be moderately salt sensitive, with several studies evaluating lettuce–salinity interaction (e.g., Kim, Fonseca, Choi, Kubota, & Kwon, 2008; Pérez-López et al., 2015; Pérez-López, Miranda-Apodaca, Munõz-Rueda, & Mena-Petite, 2013). Furthermore, green leafy vegetables, especially lettuce, contain very high nitrate levels, and above certain thresholds may lead to pathogen infection in humans (Liu, Sung, Chen, & Lai, 2014).

Studies utilizing spectroscopy to monitor lettuce condition have been explored in a wide range of stressors. For example, Woodhouse, Heeb, Berry, Hoshizaki, and Wood (1994) showed the potential of this technique for monitoring health conditions of excised leaves of lettuce grown hydroponically under different stress conditions (i.e., copper, zinc, nitrogen, phosphorus, potassium, drought), applied singularly. More recently, studies have focused on the determination of nitrogen content of lettuce leaves and canopy by spectra using multivariate modeling methods (Gao, Mao, & Zhang, 2015; Itoh et al., 2015; Mao, Gao, Zhang, & Kumi, 2015; Sun et al., 2013). A similar approach has been used to predict pigment (chlorophyll, carotenoid, anthocyanin) content in lettuce based on VIS-NIR spectroscopy (Neto et al., 2017), as well as using spectral indices (Gazula, Kleinhenz, Scheerens, & Ling, 2007; Lopes et al., 2017; Xue & Yang, 2009). Lara et al. (2016) used hyperspectral imaging to evaluate the effect of irrigation water salinity in lettuce proposing two models based on a principal component analysis of spectra and on a specifically developed vegetation index. Spectroscopy has also been used to distinguish lettuce from weeds (Slaughter, Giles, Fennimore, & Smith, 2008), and for lettuce postharvest classification (e.g., Mo et al., 2015; Moura et al., 2016). To the best of our knowledge, however, no study has explored the capacity of spectroscopy to evaluate the responses of lettuce growing under the combination of different, multiple environmental factors, as occurs both in controlled and uncontrolled environments, or combining the different analytical approaches to exploit spectral data (i.e., spectral indices, PLSR-derived traits, hyperspectral phenotyping), a gap we address in this research.

Here, we test the capability of reflectance spectroscopy to rapidly and non-destructively characterize the responses of asymptomatic, container-grown lettuce plants under the combination of different supplemental light types and intensities, and fertilization and salinity levels. Specifically, the purposes of this study were (a) to evaluate the potential of hyperspectral phenotyping to accurately detect and predict stress responses pre-visually in a multi-stress experimental design; (b) to develop spectroscopic models for the estimation of chlorophyll content, osmotic potential and total phenol concentration, three key traits for the evaluation of crop productivity and quality; and (c) to assess the variations of spectra-derived leaf traits, using both vegetation indices and traits derived from PLSR-models, under the different environmental conditions.

2 | MATERIALS AND METHODS

2.1 | Plant material and experimental design

Experimental activities were conducted in the Whistler Agriculture Research Greenhouse (40°25′21″N, 86°54′56″W, 189 m a.s.l.) at Purdue University, West Lafayette, IN. On 6 November 2017, heirloom seeds of “Salad Bowl Green” lettuce (Eden Brothers) were sown in plastic trays (27 × 54 × 7 cm) containing a Fafard Propagation Mix (Sun Gro Horticulture Inc.), following seed distributor recommendations. Seedlings emerged 3 days after plantation. On 20 November 2017, 120 seedlings were selected and individually transplanted in 0.6 L plastic pots containing the same growing mix, divided in four groups of 30 plants each, and exposed to four different supplemental light conditions (15 hr photoperiod): high-pressure sodium light (So) at low (*I*−; 318 µmol m^{-2} s^{-1} of photosynthetic active radiation, PAR) and high (*I*+; 850 µmol m^{-2} s^{-1} PAR) intensity, and tungsten light (Tu) at *I*− (175 µmol m^{-2} s^{-1} PAR) and *I*+ (425 µmol m^{-2} s^{-1} PAR). Irradiance profiles under the four supplemental light conditions at plant level are reported in Figure S1. Under each light condition, plants were daily re-positioned for the duration of the experiment to avoid position effects. On 3 December 2017, within each light group, plants were sub-divided into four groups of seven plants each and exposed to the four combinations of two levels of fertilization (*F*−; 50 ppm N, and *F*+; 150 ppm N, using 15-5-15 Peters Excel fertilizer, ICL Specialty Fertilizers) and salinity (*S*−; 0 mM NaCl, and *S*+; 200 mM NaCl), applied every other day in the watering solution (the final 200 mM NaCl concentration was reached gradually, i.e., 50, 100, 150, 200 mM on the 3, 5, 7 and 9 December 2017, respectively). Under each light condition, the two extra plants were exposed to only de-ionized water and were used only for the generation of spectral models (see below). All seedlings were kept well-watered during the whole experiment. The greenhouse day and night mean temperatures were 24 and 18°C, respectively; and maximum day and night relative humidity values were ~55% and ~50%, respectively.

On 16th December 2017, five plants from each treatment combination were selected for measurements. For four of the five plants, and for extra plants exposed to only de-ionized water, one fully expanded leaf of each plant was consecutively measured for chlorophyll content and reflectance, and were then collected as leaf portions for the determination of osmotic potential. Reflectance was also measured on a second adjacent fully expanded leaf which was then immediately frozen in liquid nitrogen and stored at −20°C until processing for total phenol analyses. The full process required <5 min per plant. The remaining plants (one plant per treatment) were measured only for reflectance on one leaf. All measurements were performed between 12.00 and 16.00 hr. Then, all measured, individual plants were separated into shoots and roots, rinsed with water, and stored at −20°C until biomass determinations.

2.2 | Standard measurements

Above- (AB) and below-ground (BB) plant biomass (dry weight, DW) were obtained after respectively drying shoots and roots at 70°C to a consistent mass. The DW of leaves used for total phenols were included in the AB determinations. A SPAD 502 meter (Minolta) was used to determine leaf chlorophyll concentration ($\mathrm{Chl}_{\mathrm{SPAD}}$). Three measurements per leaf were made and the mean of these measurements was recorded. $\mathrm{Chl}_{\mathrm{SPAD}}$ has been shown as a good representation of leaf chlorophyll content in both crop and tree species (e.g., Coste et al., 2010; Uddling, Gelang-Alfredsson, Piikki, & Pleijel, 2007). While we acknowledge the potential circularity of using a two-channel spectral index as an input for chemometric modeling, we view SPAD only as a measurement to determine chlorophyll content, and highlight that a potential outcome of this paper is the advantage of using spectral data to concomitantly estimate multiple leaf functional traits. To determine leaf osmotic potential (Ψ_π), an approximately 2 cm^2 portion of leaf was collected by a razor blade, placed in a mesh insert introduced in a microcentrifuge tube, immersed in liquid nitrogen until completely frozen and stored at −20°C until further processing. Solute concentration was determined with a vapor pressure osmometer (Wescor 5500; Wescor Inc.). Total phenol (Phen) contents were quantified colorimetrically according to Ainsworth and Gillepsie (2007) with minor modifications. Twenty mg of freeze-dried leaf samples were extracted with 1.9 ml of 95% (vol/vol) methanol at room temperature for 48 hr in the dark. Extracts were centrifuged for 5 min at 13,000 *g* and room temperature. Thereafter, 100 µl of each sample supernatant was mixed with 200 µl of 10% (vol/vol) Folin–Ciocalteu reagent and 800 µl of 700 mM $\mathrm{Na_2CO_3}$. After a 2-hr incubation at room temperature, 200 µl of each sample was transferred in a clear 96-well microplate and absorbance of each sample was recorded at 765 nm using a microplate reader (SpectraMax 190, Molecular Devices). The blank-corrected absorbances were quantified using a gallic acid standard curve (0–0.7 mg/ml) and are reported as gallic acid (GA) equivalents.

2.3 | Collection of leaf spectra

Full range (350 − 2,500 nm) reflectance profiles of lettuce leaves were collected using a SVC-1024i spectroradiometer (Spectral Vista Corporation) using a leaf-clip with an internal halogen light source attached to a plant probe. Measurements were made on two areas of the adaxial surface for each leaf, with one measurement per area, and measurements were combined to produce an average leaf spectrum. The relative reflectance of each leaf was determined from the measurement of leaf radiance divided by the radiance of a white reference panel, measured every 12 spectral collections.

2.4 | Model calibration and validation

We generated models to predict Ψ_π, $\mathrm{Chl}_{\mathrm{SPAD}}$ and Phen from untransformed reflectance profiles using PLSR (Wold et al., 2001). When predictor variables are highly correlated, as in the case with hyperspectral data, classical regression techniques can produce unreliable coefficients and error estimates (Grossman et al., 1996). In contrast to standard regression techniques, PLSR reduces a large number of collinear predictor variables into relatively few, uncorrelated latent variables, and has become the preferred method for chemometric approaches (Atzberger, Guerif, Baret, & Werner, 2010; Bolster, Martin, & Aber, 1996; Cotrozzi et al., 2018; Couture et al., 2016). To avoid potential overfitting the PLSR-model, the number of latent variables used was based on reduction of the predicted residual sum of squares statistic (Chen, Hong, Harris, & Sharkey, 2004) using leave-one-out cross-validation. Once minimized, the final set of extracted components was combined into a linear model predicting leaf traits based on leaf spectral profiles.

Model performance was evaluated by conducting 500 randomized permutations of the data sets using 80% of the data for calibration and the remaining 20% for cross validation. For each permutation, we tracked the model goodness-fit (R^2), the overall error rate (RMSE, root-mean-square error), the percentage of error over the data range (%RMSE) and bias to assess model performance when applied to the cross-validated data set. These randomized analyses generated a distribution of fit statistics allowing for the assessment of model stability as well as uncertainty in model predictions. We further determined the strength contribution of PLSR loadings by individual wavelengths using the variable important to the projection (VIP) selection statistic. The VIP statistic evaluates the importance of individual wavelengths in explaining the variation in both the response and predictor variables, with larger weightings conferring greater value to contribution of individual wavelengths to the predictive model (Chong & Jun, 2005; Wold et al., 2001).

Before running the final modeling, we developed preliminary models to identify poorly predicted outliers likely due to spectral errors, detectable from elevated reflectance in the VIS wavelengths or spectral jumps in the NIR region that occur when the leaf clip is not fully closed on either the reference or target measurements, and/or reference measurement errors (Cotrozzi et al., 2018; Couture et al., 2016). Outliers removed accounted for ca. 10% of the initial data.

The modeling approach and data analyses were performed using the "pls" package in R (www.r-project.org).

2.5 | Spectral indices and prediction of leaf traits

We calculated commonly used spectral indices: PRI, $(R_{531} - R_{570})/(R_{531} + R_{570})$ (Gamon et al., 1997; in order to avoid negative values of PRI, values were scaled as sPRI = (PRI + 1)/2 as reported by Letts, Phelan, Johnson, & Rood, 2008) and NDWI, $(R_{857} - R_{1241})/(R_{857} + R_{1241})$ (Gao, 1996). R_x indicates reflectance at x nm wavelength. Leaf mass per area (LMA, g DW/m^2), and foliar carbon (C) and nitrogen (N) concentrations (%DW) were generated from spectra using calibrations from Serbin (2012). Ψ_π (MPa), $\mathrm{Chl}_{\mathrm{SPAD}}$ and Phen (mg GA/g DW) values were generated from spectra using PLSR-models reported above, and samples removed in PLSR-modeling were not included. All spectral indices and leaf traits were predicted from spectra averaged per plant.

2.6 | Statistical analyses

We determined the influence of supplemental light type (*L*), supplemental light intensity (*I*), fertilization (*F*), salinity (*S*) and their interactions on the reflectance profiles of lettuce (averaged per plant) using permutational multivariate analysis of variance (PERMANOVA; Anderson, 2001), employing Euclidian measurements of dissimilarity and 10,000 permutations. Spectral responses were visualized conducting principal coordinates analysis (PCoA) on the same spectral data utilized for PERMANOVA, using the "vegan" package in R (www.r-project.org; Dixon, 2003). This method uses a distance of uncorrelated variables, or principal coordinates, reducing the dimensionality of the data. Using Euclidian distances, PCoA was performed for the significant factors and interactions shown by PERMANOVA.

Using only the spectral profiles that showed statistically significant separation using PERMANOVA, we additionally used PLS discriminant analysis (PLS-DA; Chevallier, Bertand, Kohler, & Courcoux, 2006) to determine the ability of spectral data to classify lettuce environmental stress. PLS-DA is a statistical approach used with high dimensional data to discriminate groups by projecting latent variables through the response and predictor variables to both reduce data dimensionality and maximize prediction accuracy and is an appropriate method for data in which predictor variables have a high degree of collinearity (Couture et al., 2018). The PLS model fits response variables that are indicators of groups of interest to the spectrum. In this study, we focused on the spectral regions which showed the higher differences among environmental conditions as determined by PERMANOVA. The analyses were applied by using a 500-times-jackknifed splitting of observations into different groups of training (calibration) and resting (validation) sets. We used the number of correct classifications both in the calibration and the validation sets across 500 iterations to evaluate the accuracy of the tested model. The calibration: validation data ratio and the number of components call to get the models that would give the best fit to the data were determined by iteratively running the PLS-DA models with different calibration: validation data ratio (i.e., 50:50, 70:30, 80:20) and numbers of components and was based on the highest kappa values returned for the validation models. PLS-DA modeling was performed using the "caret" and "vegan" packages in R (www.r-project.org; Dixon, 2003; Kuhn, 2008).

We analyzed leaf traits by four-way ANOVA following the model $y_{ij} = \mu + L_i + I_j + F_k + S_l + LI_{ij} + LF_{ik} + LS_{il} + IF_{jk} + IS_{jl} + FS_{kl} + LIF_{ijk} + LIS_{ijl} + LFS_{ikl} + LIFS_{jkl} + e_{ijkl}$. In this model, μ represents the mean, *L* represents supplemental light type *i*, *I* represents supplemental light intensity *j*, *F* represents fertilization *k*, *S* represents salinity *l*, and e_{ijkl} represents the error term. Comparisons among means were determined by the Fisher's least significant difference post hoc test. Relations among predicted leaf traits were evaluated using Pearson's correlations. Statistical analyses were preceded by examination of residuals by the Shapiro–Wilk *W* test which confirmed that data met the assumption of normality. Effects with $p < .05$ were considered statistically significant, while effects with $p < .095$ were described as marginally significant. Statistical analyses were performed in either JMP 13.2.0 (SAS Institute Inc.) or R (www-r-project.org).

3 | RESULTS

3.1 | Hyperspectral phenotyping

We initially examined multiple different wavelength ranges to optimize PERMANOVA statistical outputs (Table S1). Final PERMANOVA utilized the wavelength ranges 400–800 nm and 1,900–2,200 nm, and its output is reported in Table 1. PERMANOVA revealed that *L*, *I* and *S* affected the reflectance profile of lettuce leaves. Significant interactions were also observed for the interactions *L* × *I*, *L* × *S* (marginally significant, $p = .091$), and for *L* × *F* × *S* (Figure 1). The best classifications of environmental conditions from spectra (higher mean Kappa) were found with a 80:20 ratio for calibration:validation data using 9, 10, 9, 15, 10 and 17 components for *L*, *I*, *S*, *L* × *I*, *L* × *S*, and *L* × *F* × *S*, respectively (Table S2). Unifactorial conditions were most accurately classified from spectra (mean overall accuracy and kappa were 0.76 and 0.52 for *L*; 0.87 and 0.74 for *I*; and 0.91 and 0.82 for *S*), while modest classification outputs were found for bifactorial conditions (0.64 and 0.52, and 0.61 and 0.48 for *L* × *I* and *L* × *S*, respectively), and scarce for *L* × *F* × *S* (0.33 and 0.24, Table 2).

3.2 | Predictions of leaf traits

We initially examined numerous models containing multiple different wavelength ranges and components to optimize model performance (Table S3). Final models for Ψ_π, $\mathrm{Chl}_{\mathrm{SPAD}}$ and Phen utilized the wavelength ranges 950–2,400 nm, 500–900 nm and 1,100–2,400 nm, and included 11, 9 and 9 components, respectively. Ψ_π, $\mathrm{Chl}_{\mathrm{SPAD}}$ and Phen were well predicted from spectral data collected from leaves of lettuce under different environmental

TABLE 1 *p* values of four-way permutational analysis of variance for the effects of supplemental light type (*L*), supplemental light intensity (*I*), fertilization (*F*), salinity (*S*) and their interactions on reflectance profiles (400–800 nm + 1,900–2,200 nm) of lettuce leaves

Treatment combinations	*df*	*p*
L	1	**<.001**
I	1	**<.001**
F	1	.758
S	1	**<.001**
L × *I*	1	**.009**
L × *F*	1	.128
L × *S*	1	*.091*
I × *F*	1	.254
I × *S*	1	.794
F × *S*	1	.945
L × *I* × *F*	1	.749
L × *I* × *S*	1	.713
L × *F* × *S*	1	**.048**
I × *F* × *S*	1	.829
L × *I* × *F* × *S*	1	.457

Note: df represents the degrees of freedom. Significant values ($p < .05$) are shown in bold and marginally significant values ($p < .095$) are shown in italics.

conditions. Mean cross validation values for Ψ_π were $R^2 = 0.75$, RMSE = 0.30 MPa, bias = 0.00, and %RMSE = 9%; for Chl_{SPAD} are $R^2 = 0.84$, RMSE = 0.61, bias = 0.05, and %RMSE = 8%; and for Phen are $R^2 = 0.70$, RMSE = 1.80, bias = −0.03, and %RMSE = 13% (Figure 2a,c,e). Ψ_π standardized coefficients and VIP values highlighted important wavelengths around 1,400 nm and in the 1,850–2,100 nm range (Figure 2b). Chl_{SPAD} standardized coefficients were most pronounced in the 500–700 nm spectral region and over 850 nm, although Chl_{SPAD} VIP did not highlight specific wavelengths throughout the selected spectral region (Figure 2d). Standardized coefficients of Phen peaked around 1,400, 1,500, 1,600, 1,800, 1,900 and 2,100 nm, and VIP profile of Phen highlighted important wavelengths around 1,400 and 1,900 nm (Figure 2f).

3.3 | Variations of leaf traits

Statistical outputs for variations of observed reference (4 replications) and spectra predicted (5 replications, reported below) traits were similar (*data not shown*). We found a significant four-way interaction, *L* × *I* × *F* × *S*, on AB (Table 3). Higher AB values were found for plants under So, *I*+, *F*− and *S*+; So, *I*+, *F*+ and *S*−; and Tu, *I*+, *F*+ and *S*−. Lower values of AB were found for plants exposed to *I*− and *S*+, regardless of the light type and fertilization level (Figure 3a). Significant interactions were also observed for *L* × *S*, *I* × *F* (marginally significant, $p = .089$), *I* × *S*, and *F* × *S* for AB:BB which showed (a) higher values under Tu and *S*−, and lower values under Tu and *S*+; (b) lower values under *I*+ and *F*−; (c) higher values under *I*− and *S*−, and lower values under *I*+ and *S*+; and (d) higher values under *F*+ and *S*−, and lower values under *F*− and *S*− (Table 3, Figure 3b). We also found a marginally significant *L* × *I* × *F* × *S* interaction on sPRI ($p = .093$, Table 3) which was lower for plants under So at *I*+, especially in the co-occurring presence of *F*+ and *S*+ (Figure 3c). *L* × *I* and *L* × *S* interactions were significant on NDWI (Table 3). Higher values were found (a) under So at *I*+, followed by Tu at *I*+; and (b) under So and *S*+, followed by Tu and *S*+ (Figure 3d). Two significant three-way interactions, *L* × *I* × *S* and *I* × *F* × *S*, were observed on Ψ_π (Table 3). Ψ_π dropped due to *S*+, especially under (a) So at *I*+, followed by Tu at *I*+ and Tu at *I*−, and then So at *I*−; or (b) *I*+ and *F*+, followed by *I*+ and *F*−, and then *I*− and *F*−, and *I*− and *F*+ (Figure 3e). We found a significant *L* × *F* interaction on Chl_{SPAD} with higher values under Tu and *F*− and lower values under So and *F*−. Chl_{SPAD} also increased under *S*+, overall (Table 3, Figure 3f). Significant interactions of *L* × *I*, *L* × *S*, and *F* × *S* were found on LMA. Higher levels of LMA were found under (a) So at *I*+, followed by Tu at *I*+, then Tu at *I*−, and finally So at *I*−; (b) Tu or So and *S*+, followed by So and *S*−, and finally Tu and *S*−; and (c) *F*+ and *S*+, followed by *F*− and *S*+, and finally *F*− or *F*+ and *S*− (Table 3, Figure 3g). We also found significant three-way significant interactions, *L* × *I* × *S* and *L* × *F* × *S* (marginally significant, $p = .070$), on N (Table 3). N levels were (a) higher under *I*−, especially for Tu and *S*−, while lower under *I*+, especially for So, and even more in concomitance of *S*+; and (b) higher under Tu, *F*− and *S*−, Tu, *F*+ and *S*−, and So, *F*+ and *S*−, in comparison to all the other conditions which showed similar values (Figure 3h). A significant *L* × *I* × *S* interaction was observed on C:N (Table 3). Higher C:N values occurred under *I*+, especially for So and *S*+, followed by So and *S*−, while under *I*−, higher values were observed under Tu and *S*+ (Table 3, Figure 3i). We finally found a marginally significant *L* × *I* × *F* interaction ($p = .066$) on Phen, while *S* showed significant binary interactions with the other factors: *L* × *S* (marginally significant: $p = .064$), *I* × *S* and *F* × *S* (Table 3). Phen levels were (a) higher under So at *I*+, regardless of the fertilization regime, while lower under So at *I*− and *F*+, and under Tu at *I*−, regardless of the fertilization regime; (b) higher under So and *S*−, followed by Tu and *S*−, then So and *S*+, and finally Tu and *S*+; (c) higher under *I*+ and *S*−, followed by *I*− and *S*−, then *I*+ and *S*+, and finally *I*− and *S*+; and (4) higher under *F*− and *S*−, followed by *F*+ and *S*−, and finally *F*+ or *F*− and *S*+ (Figure 3j).

3.4 | Correlations among leaf traits

sPRI was positively related to Chl_{SPAD} and N, and negatively related to NDWI, LMA, and C:N (Table 4). NDWI was also positively related to LMA and C:N, and negatively related with Ψ_π and N (Table 4). Here Ψ_π was also positively related to N and Phen, and negatively related to LMA and C:N (Table 4). Chl_{SPAD} was also negatively related to Phen (Table 4). LMA was positively related to C:N, and negatively related to N, while N was negatively related to C:N (Table 4).

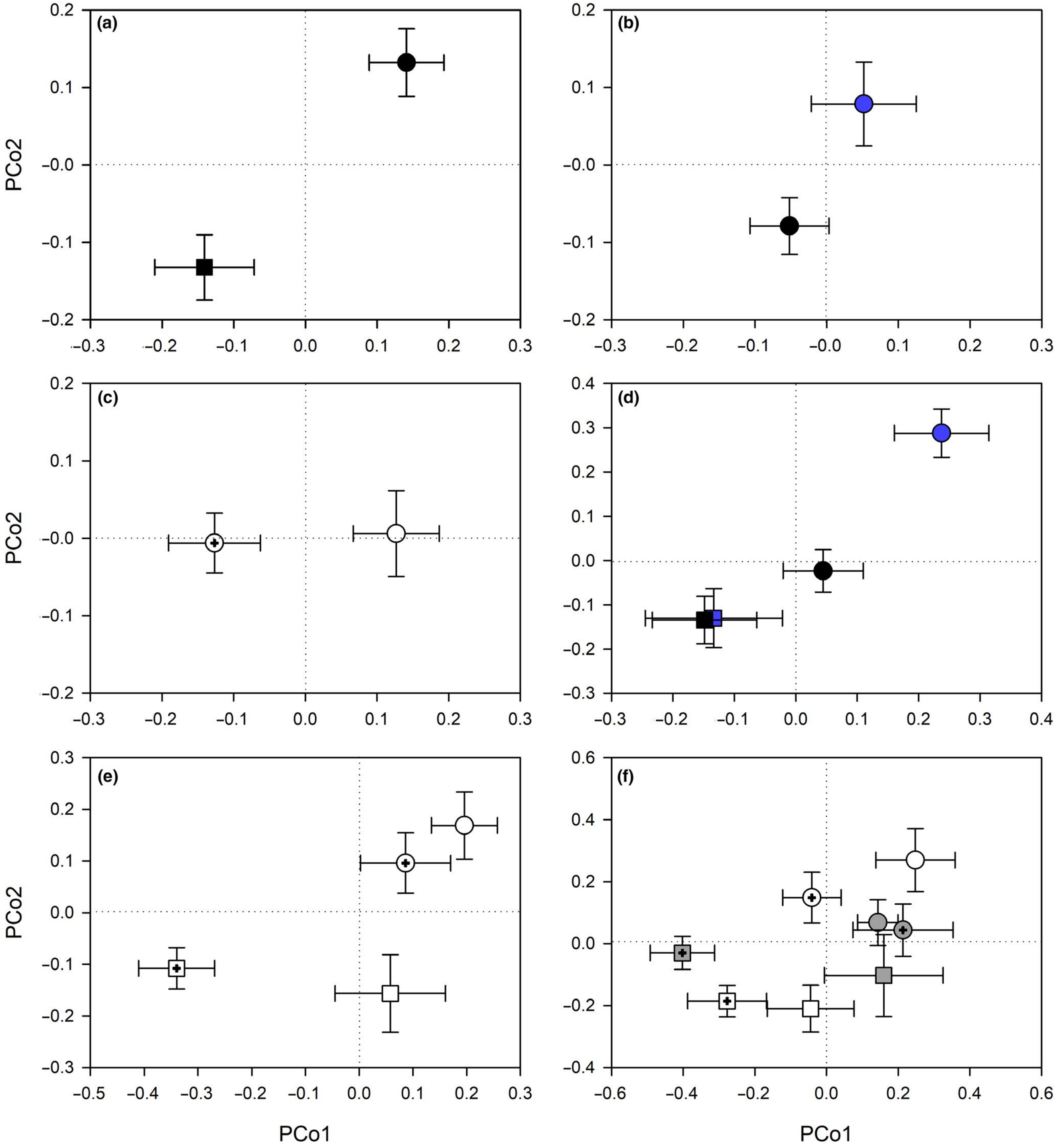

FIGURE 1 Scores ($M \pm SE$) for the first and second principal components from principal coordinates analysis (PCoA) of reflectance data (400–800 nm and 1,900–2,200 nm) collected from lettuce leaves, highlighting the ability of spectroscopy to detect the effects of supplemental light type (a); supplemental light intensity (b); salinity (c); supplemental light type × supplemental light intensity (d); supplemental light type × salinity (e); and supplemental light type × fertilization ×salinity (f). *Circle symbols*: sodium light; *square symbols*: tungsten light; *black symbols*: low light intensity; *blue symbols*: high light intensity; *empty symbols*: no salinity; *crossed symbols*: salinity; *white symbols*: low fertilization; *gray symbols*: high fertilization

4 | DISCUSSION

Advancements in the ability to rapidly detect plant responses to environmental stress is necessary to improve crop management practices and to meet the 21st century challenge for increasing global food demand (Mickelbart et al., 2015). Here, we show the ability of spectroscopy to simultaneously provide morphological, physiological and biochemical information regarding multiple plant

TABLE 2 Number of components (Comps), accuracy, 95% confidential interval (CI) of accuracy and kappa for cross validation data generated via partial least squares discriminant analysis, using 80% of the data for calibration and 20% for cross validation, for the classification of supplemental light type (*L*), supplemental light intensity (*I*), salinity (*S*), *L* × *I*, *L* × *S*, and *L* × fertilization (*F*) × *S* conditions from lettuce spectra (400–800 nm + 1,900–2,200 nm)

Treatment combination	Comps	Accuracy, %	95% CI accuracy	κ
L	9	0.76	0.50–0.93	0.52 ± 0.01
I	10	0.87	0.62–0.97	0.74 ± 0.01
S	9	0.91	0.67–0.99	0.82 ± 0.01
L × *I*	15	0.64	0.38–0.85	0.52 ± 0.01
L × *S*	10	0.61%	0.35–0.83	0.48 ± 0.01
L × *F* × *S*	17	0.33	0.13–0.60	0.24 ± 0.01

Note: Data are shown as *M* ± *SE* from 500 simulated models.

constituents with a single spectral measurement. We specifically demonstrate that spectroscopic data can be used to effectively monitor and detect interactive effects of multiple environmental factors (i.e., supplemental light type, supplemental light intensity, fertilization and salinity) on lettuce health, quality and yield, but we also highlight that the approach may have limitations, as prediction accuracies decreased as stress combinations, and environmental variation, increased.

Spectra are themselves an overall expression of the aggregate signals of physiological, morphological and biochemical properties of leaves under different environmental conditions. Thus, utilization of hyperspectral data may prevent loss of information, resulting from relying on solely standard measurement approaches, that could be meaningful, providing information about a comprehensive ensemble of traits (i.e., spectral phenotyping), including those that we may not have measured or we may not yet know are important (Cavender-Bares et al., 2016). Spectra may, thus, represent a more powerful approach than direct measurements of leaf traits to monitor crop status.

The most innovative outcome of the current study comes from using this approach: we showed that reflectance profiles of lettuce leaves were sensitive to different environmental conditions. At an early developmental stage and asymptomatically (i.e., visible symptoms were not observed), we were able to distinguish lettuce individuals grown under different supplemental light type and intensity or salt conditions, using the spectral regions from 400 to 800 nm and from 1,900 to 2,200 nm. This outcome is particularly interesting for lettuce since the quality and yield of this species are particularly sensitive to light conditions (Saito et al., 2010; Samoulienė et al., 2012; Wang et al., 2016) and salinity (Kim et al., 2008; Pérez-López et al., 2015, 2013). We also identified specific spectral markers to discriminate the effects of different binary combinations *L* × *I* and *L* × *S* (although their interaction was marginally significant), as well as of the combination of *L* × *F* × *S*, although *F* alone did not affect spectral profiles. The 400–800 nm region was likely important for the detection of the effects of the four environmental factors on photosynthetic metabolism and photochemical apparatus, which are known to be affected in these stress environments (Guidi et al., 2017; Johkan, Shoji, Goto, Hahida, & Yoshihara, 2012; Sun, Ye, Peng, & Li, 2016). This region includes leaf pigment absorption wavelengths (Merzlyak, Gitelson, Chivkunova, Solovchenko, & Pogosyan, 2003), as well as the red-edge (700–750 nm; Mutanga & Skidmore, 2007). The importance of these spectral features in the assessment of the photosynthetic processes has been previously reported for several plant species (e.g., Gamon et al., 1997; Merzlyak et al., 2003; Serbin, Dillaway, Kruger, & Townsend, 2012; Yendrek et al., 2017), and numerous studies have also shown that the shape of the red-edge is dependent on chlorophyll content (Clevers, Kooistra, & Salas, 2004; Filella & Peñuelas, 1994; Smith, Steven, & Colls, 2004; Zarco-Tejada, Miller, Morales, Berjón, & Agüera, 2004) and stress conditions (Cotrozzi et al., 2018; Mutanga & Skidmore, 2007; Smith et al., 2004).

The 1,900–2,200 nm range was, instead, likely important for the detection of other key regulations adopted by plants to adjust to environmental constrains. The osmotic adjustment necessary under salinity and other stress can lead to an accumulation of compatible solutes and ion in the vacuole (Guidi et al., 2017; Romero-Aranda, Soria, & Cuartero, 2001), and multiple studies (Asner & Martin, 2015; Cotrozzi et al., 2017; Ramirez et al., 2015; Rubert-Nason et al., 2013; Shetty & Gislum, 2011) have reported that wavelengths important for predicting non-structural carbohydrates and other foliar osmolyte concentrations using spectroscopy are within the 1,900–2,250 nm range. Plant secondary metabolites also play critical roles in plant functioning and greatly contribute to phytochemical diversity, and reflectance spectroscopy has also been used to estimate concentrations of the major groups of secondary compounds including alkaloids, glucosinolates, terpenoids, phenylpropanoids and related phenolic compounds (Carvalho et al., 2013; Couture et al., 2013, 2016; Ebbers, Wallis, Dury, Floyd, & Foley, 2002; Font, Río-Celstino, Rosa, Aires, & Haro-Balión, 2005; Kokaly & Skidmore, 2015; Rubert-Nason et al., 2013; Schulz, Engelhardt, Wegent, Drews, & Lapczynski, 1999), highlighting again specific absorption features within the 1,900–2,250 nm range. This spectral region also contains the main protein absorption features (Curran, 1989), suggesting that it is important in the detection of the *L* × *F* × *S* interaction. These outcomes clearly highlight the huge potential of reflectance spectroscopy in crop phenotyping and management. The incapability we found in detecting the four-way *L* × *I* × *F* × *S* interactive effect on spectra profiles as well as the reduced classification accuracy with increasing statistic factors was likely due to the heterogeneous responses induced by the variable environmental conditions and the low treatment replication. Better outputs might be reached by increasing the experimental replications; this is especially true in field settings, where growing conditions can be highly variable.

In this study, we also present a robust approach by which specific plant physiological and biochemical responses to different combinations of abiotic stress environments can be monitored using reflectance spectroscopy and that utilizes multiple permutation of the data, providing explicit estimates of model uncertainty. Ψ_π, $\mathrm{Chl}_{\mathrm{SPAD}}$

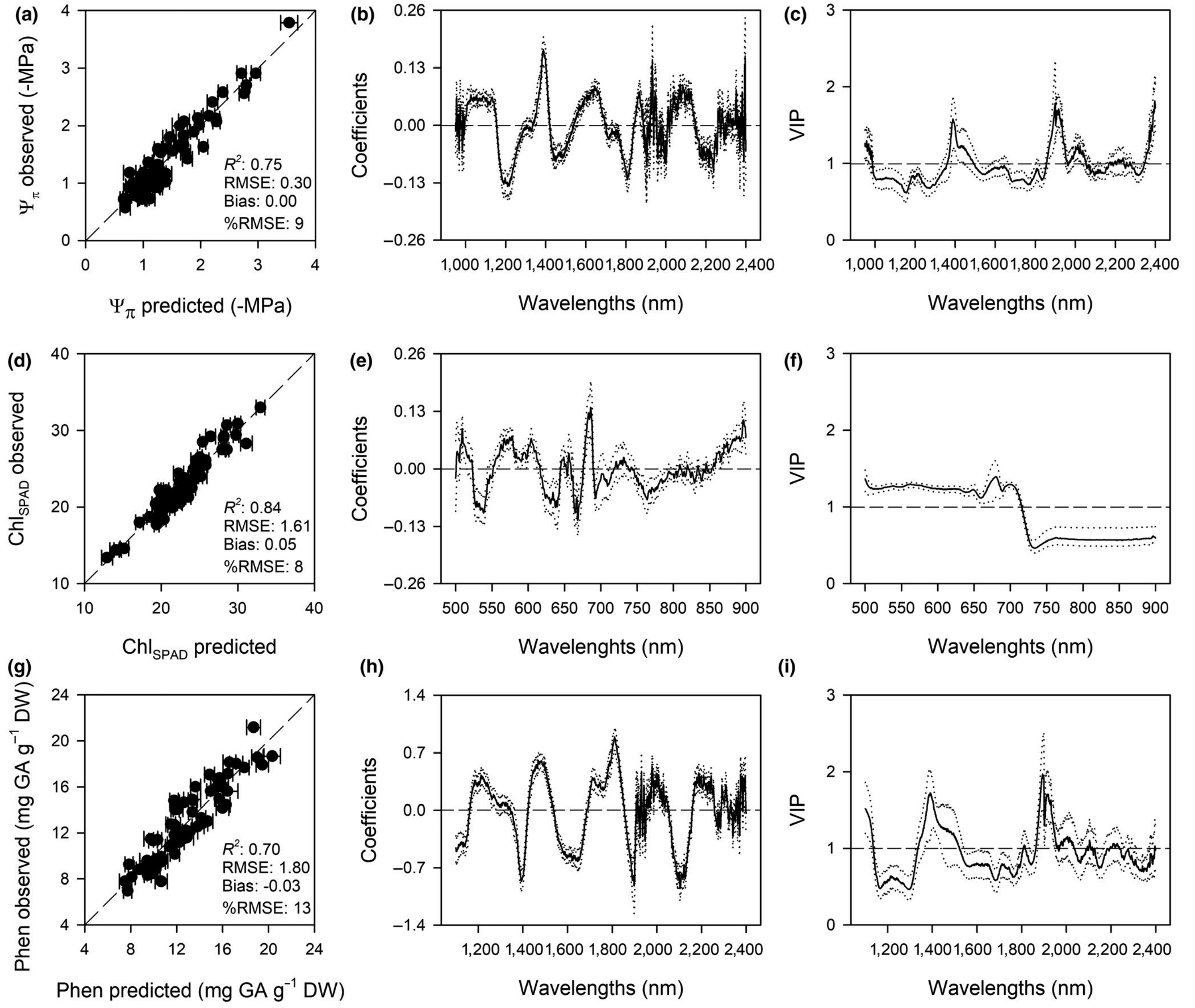

FIGURE 2 (a,d,g) Observed versus partial least squares regression (PLSR)-predicted values of osmotic potential (Ψ_π), chlorophyll content (Chl_{SPAD}) and total phenols (Phen) in lettuce; error bars for predicted values represent the standard deviations generated from 500 simulated models; dashed line is 1:1 relationship; model goodness-fit (R^2), root-mean-square error (RMSE), bias and %RMSE for cross validation data generated using 80% of the data for calibration and 20% for cross validation are reported. (b,e,h) Mean (solid), 5th and 95th percentile (dotted) of standardized coefficients and (c,f,i) variable importance for projection values (VIP) by wavelengths for PLSR-models predicting Ψ_π, Chl_{SPAD} and Phen in lettuce

and Phen were well predicted by spectral data (R^2 for cross validation: 0.75, 0.84 and 0.70, respectively). We found that the spectral region for the best prediction of Ψ_π was 950–2,400 nm. This wavelength range included the minor water absorption features centered at 970 and 1,200 nm as well as those of known osmolytes likely involved in osmotic regulation (Cotrozzi et al., 2017) in the prediction of Ψ_π in lettuce leaves. Chl_{SPAD} is an index based on the absorbance of the leaf at two specific wavelengths (i.e., 650 and 940 nm), and in accordance with these wavelength ranges, Chl_{SPAD} was best predicted using the 500–900 nm, including both the pigment absorption features and the red-edge. Chl_{SPAD} modeling outputs are in accordance with the prediction of Chl content in lettuce by Neto et al. (2017). Also, Phen modeling, which showed the best predicting region from 1,100 to 2,400 nm, confirmed the importance of specific absorption features found in previous studies (Couture *et al.* 2016; Kokaly & Skidmore, 2015; Rubert-Nason et al., 2013). By combining high-fidelity reflectance measurements, standard physiological and biochemical analyses and robust statistical modeling, we demonstrate the potential to expand prediction capabilities of spectral data for leaf traits necessary for the early detection of plant responses when exposed to different abiotic stress environments. However, development and validation of further spectral models are required since these outcomes are potentially species- and environment specific. The prediction of these physiological and chemical responses, in combination with the hyperspectral phenotyping approach, has the potential to provide multiple layers of stress-specific information

TABLE 3 *P* values of four-way analysis of variance for the effects of supplemental light type (*L*), supplemental light intensity (*I*), fertilization (*F*), salinity (*S*) and their interactions on leaf traits of lettuce

	df	AB	AB:BB	sPRI	NDWI	Ψ_π	Chl_{SPAD}	LMA	N	C:N	Phen
L	1	**0.002**	0.858	**<0.001**	**<0.001**	0.243	**<0.001**	*0.057*	**<0.001**	**<0.001**	**<0.001**
I	1	**<0.001**	**0.024**	**<0.001**	**<0.001**	**<0.001**	0.404	**<0.001**	**<0.001**	**<0.001**	**<0.001**
F	1	0.125	**<0.001**	0.101	0.502	**0.040**	0.841	0.924	0.414	0.683	**0.002**
S	1	**<0.001**	0.628	0.955	**<0.001**	**<0.001**	**<0.001**	**<0.001**	**<0.001**	**<0.001**	**<0.001**
L × *I*	1	*0.083*	0.581	**<0.001**	**<0.001**	**0.003**	0.290	**<0.001**	**<0.001**	**<0.001**	**0.001**
L × *F*	1	**0.025**	0.281	0.779	0.391	0.400	**0.020**	0.430	*0.059*	0.109	0.134
L × *S*	1	0.780	**0.020**	**0.044**	**0.028**	0.284	0.243	**0.016**	0.420	0.244	*0.064*
I × *F*	1	**0.028**	*0.089*	0.124	0.537	0.806	0.343	0.098	*0.070*	0.237	0.289
I × *S*	1	**0.023**	**0.011**	**0.048**	0.979	**<0.001**	0.472	0.661	0.640	*0.062*	**<0.001**
F × *S*	1	**0.005**	**<0.001**	0.511	0.859	0.536	0.805	**0.007**	0.420	0.431	**0.001**
L × *I* × *F*	1	**0.016**	0.262	0.357	0.177	0.932	0.891	0.111	0.957	0.695	*0.066*
L × *I* × *S*	1	0.386	0.213	**0.013**	0.286	**0.003**	0.965	0.347	**0.004**	**<0.001**	0.610
L × *F* × *S*	1	0.939	0.429	**0.018**	0.765	0.306	0.433	0.412	*0.070*	0.175	0.748
I × *F* × *S*	1	**0.005**	0.141	*0.073*	0.605	**0.010**	0.865	0.206	0.724	0.414	0.683
L × *I* × *F* × *S*	1	**<0.001**	0.193	*0.093*	0.913	0.312	0.406	0.278	0.507	0.948	0.703

Note: df represents the degrees of freedom. Significant values ($p < .05$) are shown in bold and marginally significant values ($p < .095$) are shown in italics.

Abbreviations of leaf traits: AB, above biomass; AB:BB, above:below biomass ratio; sPRI, photosynthetic reflectance index (scaled); NDWI, normalized difference water index; Ψ_π, osmotic potential; Chl_{SPAD}, SPAD based chlorophyll content; LMA, leaf mass per area; N, nitrogen; C:N carbon to nitrogen ratio; Phen, total phenols.

to growers, including identification of stress and the also the identification of underlying physiological responses to stress, that can increase the efficiency of management responses.

Using both standard measurements and spectra-derived leaf traits (by both indices and PLSR-models), variations of key features such as biomass production and allocation, photosynthetic performance, water status, leaf morphology, chlorophyll content, macronutrient composition, and phenolic concentration were investigated to assess stress conditions in plants exposed to the variable environments. As expected, AB, an important crop feature, was enhanced by high light intensity and fertilization, but decreased under exposure to high salinity levels. The highest AB levels were found in plants exposed to So light at *I*+, which, unexpectedly, showed high AB also in presence of *F*− and *S*+. These outcomes highlight that different combinations of stressors can differently, and non-additively, affect plant growth (Landi et al., 2019; Pandey et al., 2017; Podda et al., 2019; Zhang et al., 2018). The different AB production of lettuce under variable environmental conditions did not seem due to divergent resource allocations between shoots and roots: among the factors, salinity was the most influential on AB:BB. While plants exposed to So light at I + showed higher AB, they were also the only ones showing a lower photosynthetic radiation use efficiency (sPRI, negatively related to AB). Reduced PRI is usually associated with reduced net CO_2 uptake and the maximum efficiency of photosystem II photochemistry in the light, and increased levels of the photoprotective xanthophyll cycle pigment zeaxanthin (Gamon et al., 1997). These reductions of sPRI where confirmed by the reductions in N, and consequently by the increases of C:N. Foliar nitrogen is strongly related to the photosynthetic capacity of leaves given its role in the light harvesting pigments and photosynthetic machinery, especially the enzyme RuBisCo (Evans, 1989).

At the same time, plants exposed to So light at *I*+ had a higher water content (NDWI, positively related to AB), especially under salinity which induced a more pronounced osmoregulation compared to the other environmental conditions (Ψ_π dropped mostly). It is known that a decrease in Ψ_π is one of the main adjustments under salinity (Negrão, Schmöckel, & Tester, 2017). We can, thus, conclude that AB production of lettuce leaves was more affected by the amount of water than the photosynthetic performance, although these physiological processes seemed to be partially connected by a negative relationship. This interpretation was partially supported by the highest levels of Chl content found in plants exposed to Tu light or *S*+, which overall showed lower levels of AB. The increase of Chl content under *S*+ has been previously reported on several lettuce genotypes (Xu & Mou, 2015). The lack of a light intensity effect on Chl content, actually, leads us to interpret the decrease of sPRI in plants under SO light at *I*+ as a photosynthetic regulation to prevent oxidative damage (Foyer & Shigeoka, 2011) instead as an impairment of the photosynthetic apparatus.

Leaf thickness was strongly and positively related to water content (*r* = .75), as the effects induced by the interactions of light with light intensity or salt on LMA were similar to the ones on NDWI, although only LMA also showed a significant *F* × *S* interaction. Taking into account these three significant binary-combinations on LMA, we can conclude that plants under So light were more sensitive to light intensity (*I*−: lowest thickness; *I*+: highest thickness); whereas

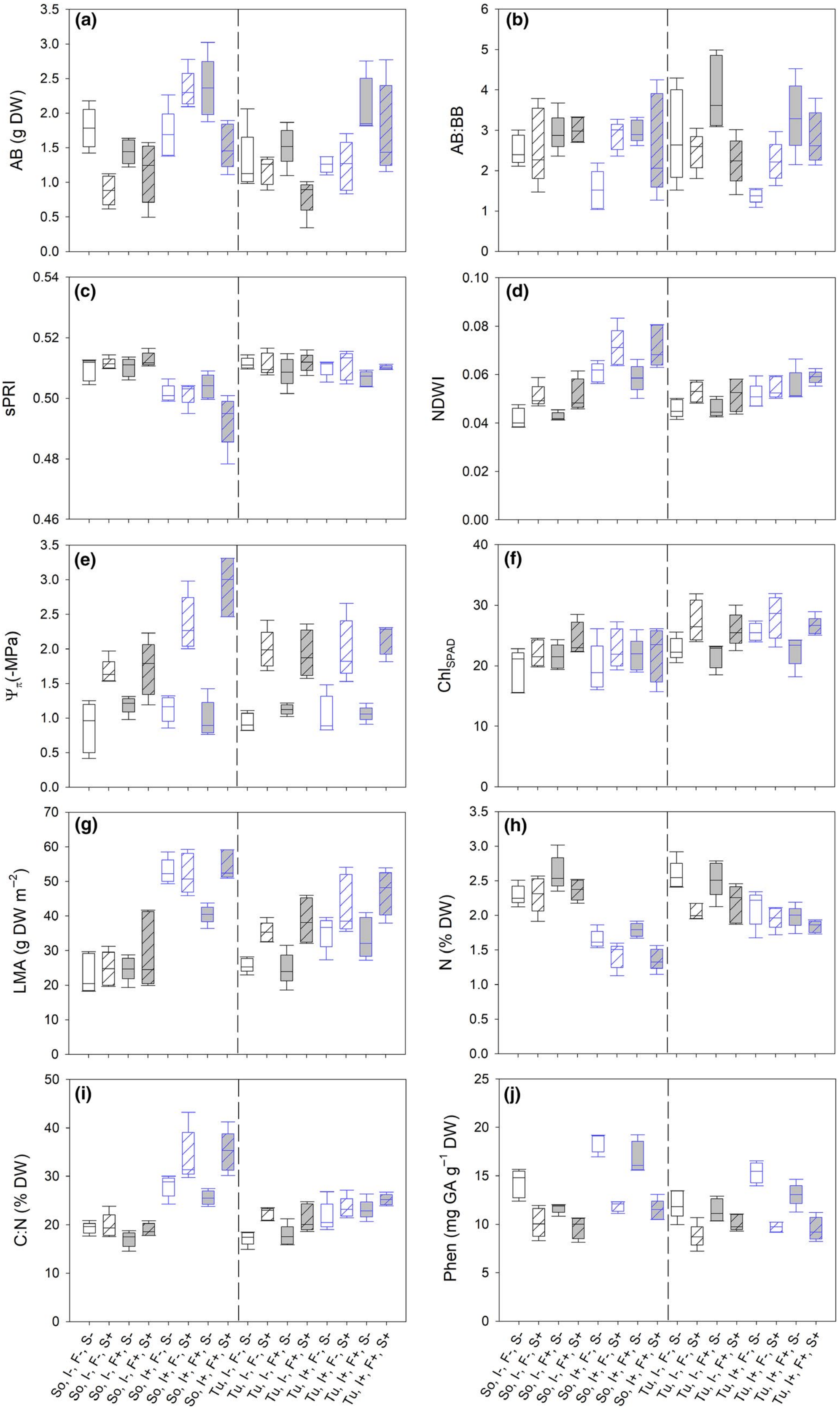

FIGURE 3 Variation in leaf traits of lettuce exposed to different supplemental light types (sodium, So, *left side*; tungsten, Tu, *right side*), supplemental light intensities (low, *I*−, *black lines*; high, *I*+, *blue lines*), fertilization (low, *F*−, *white fill*; high, *F*+, *gray fill*) and salinity (no salt, *S*−, *no pattern*; salt, *S*+, *pattern*). The box plots display the median for each trait by treatment (*horizontal line*), the 5th and 95th percentiles (*boxes*) and the range (*whiskers*). For abbreviations of leaf traits see Table 3

TABLE 4 Pearson's correlation matrix describing relationships among spectral-predicted leaf traits of lettuce

	AB	AB:BB	sPRI	NDWI	Ψ_π	Chl_{SPAD}	LMA	N	C:N
AB:BB	*0.33*								
sPRI	*−0.38*	0.06							
NDWI	0.24	−0.13	***−0.63***						
Ψ_π	*0.25*	0.13	*0.28*	***−0.64***					
Chl_{SPAD}	*−0.28*	−0.14	***0.51***	0.09	*−0.37*				
LMA	0.22	*−0.37*	***−0.54***	***0.76***	***−0.55***	0.22			
N	*−0.33*	*0.27*	***0.68***	***−0.86***	***0.51***	0.01	***−0.83***		
C:N	*0.33*	−0.21	***−0.77***	***0.90***	***−0.59***	−0.06	***0.83***	***−0.95***	
Phen	***0.41***	−0.24	*−0.35*	0.10	***0.51***	***−0.45***	0.15	*−0.25*	0.20

Note: Significant values (p < .05) are italicized. Significant correlations (r > .4) are bolded.

Abbreviations of leaf traits: AB, above biomass; AB:BB, above:below biomass ratio; sPRI, photosynthetic reflectance index (scaled); NDWI, normalized difference water index; Ψ_π, osmotic potential; Chl_{SPAD}, SPAD based chlorophyll content; LMA, leaf mass per area; N, nitrogen; C:N carbon to nitrogen ratio; Phen, total phenols.

plants under Tu light were more sensitive to salinity (*S*−: medium-low thickness; *S*+: medium-high thickness), although also for these plants was found a light intensity effect opposite to plants exposed to So light. Finally, Phen, compounds that have a great interest for their consumer health properties due to their antioxidant capacity (Hollman, 2001), decreased under *S*+, while were triggered under high light intensity, especially So type light, and low fertilization. Similar and contrasting results have been reported on lettuce phenols under salinity (Kim et al., 2008; Pérez-López et al., 2015; Sgherri et al., 2017) While we are unsure of the mechanism explaining high growth of lettuce under Tu light at *I*+, *F*+ and *S*−, we suggest that spectral data can affirm that chemical, anatomical, and physiological responses to So, *I*+, *F*+, *S*− environmental conditions that increased both the productivity and quality of lettuce.

In conclusion, we found that hyperspectral information successfully identified crop status in multi-factor experiments and detected specific responses to stress conditions prior to the onset of visual symptoms. In addition, a novel application of the hyperspectral data, we present is the non-destructive, rapid, and concomitant quantification of specific physiological, morphological, and biochemical responses of lettuce plants under variable environmental conditions. Outcomes and approaches presented in this study could have applications in numerous scientific fields (e.g., precision agriculture, robotic monitoring, plant phenotyping) with benefits not only for further plant science research, but also for growers to achieve greater crop yield and quality (and incomes), with lower environmental impact. While this approach can help to monitor plant function over large geographic regions if scaled to remote collections from air- or space-borne platforms (Cotrozzi et al., 2018), piloted and unpiloted aircraft approaches to protected agrosystems are less applicable because of the structures used for protection. In this study, however, we highlight the utility of scaled-down vegetation spectroscopy as a management and monitoring tool in a protected agrosystem and suggest that integration of this approach into intelligent and automated greenhouses and other protected systems could greatly enhance management efficiency and increase crop quality and yield.

ACKNOWLEDGEMENTS

This work was supported by USDA NIFA Hatch award IND011490 to JJC. We are grateful to Debra L. Williams for the management of the experimental activities. We thank Raquel Peron for laboratory assistance and Michael Mickelbart for access to laboratory instrumentation related to the analysis of osmotic pressure.

AUTHOR CONTRIBUTIONS

LC and JJC together planned and designed the research, performed the measurements, analyzed the data and wrote the manuscript.

ORCID

John J. Couture https://orcid.org/0000-0003-4784-4537

REFERENCES

Ainsworth, E. A., & Gillepsie, K. M. (2007). Estimation of total phenolic content and other oxidation substrates in plant tissues using Folin-Ciocalteau reagent. *Nature Protocols*, *2*, 875–877.

Anderson, M. J. (2001). A new method for non-parametric multivariate analysis of variance. *Austral Ecology*, *26*, 32–46.

Asner, G. P., & Martin, R. E. (2008). Spectral and chemical analysis of tropical forests: Scaling from leaf to canopy levels. *Remote Sensing of Environment*, *112*, 3958–3970.

Asner, G. P., & Martin, R. E. (2015). Spectroscopic remote sensing of nonstructural carbohydrates in forest canopies. *Remote Sensing*, *7*, 3526–3547.

Asner, G. P., Martin, R. E., Tupayachi, R., Emerson, R., Marinez, P., Sinca, F., … Lugo, A. E. (2011). Taxonomy and remote sensing of leaf mass per are (LMA) in humid tropical forests. *Ecological Applications*, *21*, 85–98.

Atzberger, C., Guerif, M., Baret, F., & Werner, W. (2010). Comparative analysis of three chemometric techniques for the spectrometric assessment of canopy chlorophyll content in winter wheat. *Computers and Electronics in Agriculture*, *73*, 165–173.

Bolster, K. L., Martin, M. E., & Aber, J. D. (1996). Determination of carbon fraction and nitrogen concentration in tree foliage by near infrared reflectance: A comparison of statistical methods. *Canadian Journal of Forest Research*, *26*, 590–600.

Carvalho, S., Macel, M., Schlerf, M., Moghaddam, F. E., Mulder, P. P. J., Skidmore, A. K., & Van Der Putten, W. H. (2013). Changes in plant defense chemistry (pyrrolizidine alkaloids) revealed through high-resolution spectroscopy. *ISPRS Journal of Photogrammetry and Remote Sensing*, *80*, 51–60.

Cavender-Bares, J., Meireles, J. E., Couture, J. J., Kaproth, M. A., Kingdon, C. C., Singh, A., … Townsend, P. A. (2016). Associations of leaf spectra with genetic and phylogenetic variation in oaks: Prospects for remote detection of biodiversity. *Remote Sensing*, *8*, 221.

Chen, S., Hong, X., Harris, C. J., & Sharkey, P. M. (2004). Sparse modeling using orthogonal forest regression with PRESS statistic and regularization. *IEEE Transactions on Systems, Man and Cybernetics-Part B: Cybernetics*, *34*, 898–911.

Chevallier, S., Bertand, D., Kohler, A., & Courcoux, P. (2006). Application of PLS-DA in multivariate analysis. *Journal of Chemometrics*, *20*, 221–229.

Chong, I.-G., & Jun, C.-H. (2005). Performance of some variable selection methods when multicollinearity is present. *Chemometrics and Intelligent Laboratory Systems*, *28*, 103–112.

Clevers, J. G. P. W., Kooistra, L., & Salas, E. A. L. (2004). Study of heavy metal contamination in river floodplains using the red-edge position in spectroscopic data. *International Journal of Remote Sensing*, *25*, 3883–3895.

Coste, S., Baraloto, C., Leroy, C., Marcon, È., Renaud, A., Richardson, A. D., … Hérault, B. (2010). Assessing foliar chlorophyll contents with the SPAD-502 chlorophyll meter: A calibration test with thirteen tree species of tropical rainforest in French Guiana. *Annals of Forest Science*, *67*, 607.

Cotrozzi, L., Couture, J. J., Cavender-Bares, J., Kingdon, C. C., Fallon, B., Pilz, G., … Townsend, P. A. (2017). Using foliar spectral properties to assess the effects of drought on plant water potential. *Tree Physiology*, *13*, 1582–1591.

Cotrozzi, L., & Landi, M. (2018). Molecular and physiological adaptations of tea plant in response to low light and UV stress. In W.-Y. Han, C. Li, & G. J. Ahammed (Eds.), *Stress physiology of tea in the face of climate change* (pp. 83–110). Singapore: Springer Nature Singapore Ltd.

Cotrozzi, L., Townsend, P. A., Pellegrini, E., Nali, C., & Couture, J. J. (2018). Reflectance spectroscopy: A novel approach to better understand and monitor the impact of air pollution on Mediterranean plants. *Environmental Science and Pollution Research*, *25*, 8249–8267.

Couture, J. J., & Lindroth, R. L. (2012). Atmospheric change alters performance of an invasive forest insect. *Global Change Biology*, *18*, 3543–3557.

Couture, J. J., Serbin, S. P., & Townsend, P. A. (2013). Spectroscopic sensitivity of real-time, rapidly induced phytochemical change in response to damage. *New Phytologist*, *198*, 311–319.

Couture, J. J., Singh, A., Charkowski, A. O., Groves, R. L., Gray, S. M., Bethke, P. C., & Townsend, P. A. (2018). Integrating spectroscopy with potato disease management. *Plant Disease*, *10*, 2233–2240. https://doi.org/10.1094/PDIS-01-18-0054-RE

Couture, J. J., Singh, A., Rubert-Nason, K. F., Serbin, S. P., Lindroth, R. L., & Townsend, P. A. (2016). Spectroscopic determination of ecologically relevant plant secondary metabolites. *Methods in Ecology and Evolution*, *7*, 1402–1412.

Curran, P. J. (1989). Remote sensing of foliar chemistry. *Remote Sensing of Environment*, *30*, 271–278. https://doi.org/10.1016/0034-4257(89)90069-2

DaMatta, F. M., Grandis, A., Arenque, B. C., & Buckeridge, M. S. (2010). Impacts of climate changes on crop physiology and food quality. *Food Research International*, *43*, 1814–1823. https://doi.org/10.1016/j.foodres.2009.11.001

Deacon, N. J., Grossman, J. J., Schweiger, A. K., Armour, I., & Cavender-Bares, J. (2017). Genetic, morphological, and spectral characterization of relictual Niobrara River hybrid aspens (*Populus* × *smithii*). *American Journal of Botany*, *104*, 1–13.

Dixon, P. (2003). VEGAN, a package of R functions for community ecology. *Journal of Vegetation Science*, *14*, 927–930.

Ebbers, M. J. H., Wallis, I. R., Dury, S., Floyd, R., & Foley, W. J. (2002). Spectrometric prediction of secondary metabolites and nitrogen in fresh Eucalyptus foliage: Towards remote sensing of the nutritional quality of foliage for leaf-eating marsupials. *Australian Journal of Botany*, *50*, 761–768. https://doi.org/10.1071/BT02025

Evans, J. R. (1989). Photosynthesis and nitrogen relationships in leaves of C_3 plants. *Oecologia*, *78*, 9–19. https://doi.org/10.1007/BF00377192

Filella, I., & Peñuelas, J. (1994). The red edge position and shape as indicators of plant chlorophyll content, biomass and hydric status. *International Journal of Remote Sensing*, *15*, 1459–1470.

Font, R., Del Río-Celstino, M., Rosa, E., Aires, A., & De Haro-Balión, A. (2005). Glucosinolate assessment in *Brassica oleracea* leaves by near-infrared spectroscopy. *Journal of Agricultural Sciences*, *145*, 65–73.

Foyer, C. H., & Shigeoka, S. (2011). Understanding oxidative stress and antioxidant functions to enhance photosynthesis. *Plant Physiology*, *155*, 93–100. https://doi.org/10.1104/pp.110.166181

Gamon, J. A., Serrano, L., & Surfus, J. S. (1997). The photochemical reflectance index: An optical indicator of photosynthetic radiation use efficiency across species, functional types, and nutrient levels. *Oecologia*, *112*, 492–501. https://doi.org/10.1007/s004420050337

Gao, B. C. (1996). NDWI-a normalized difference water index for remote sensing of vegetation liquid from space. *Remote Sensing of Environment*, *58*, 257–266.

Gao, H., Mao, H., & Zhang, X. (2015). Determination of lettuce nitrogen content using spectroscopy with efficient wavelength selection and extreme learning machine. *Zemdirbyste-Agriculture*, *102*, 51–58. https://doi.org/10.13080/z-a.2015.102.006

Gascuel, Q., Diretto, G., Monforte, A. J., Fortes, A. M., & Granell, A. (2017). Use of nutritional diversity and biotechnology to increase the quality and nutritional content of tomato and grape. *Frontiers in Plant Science*, *8*, 652.

Gazula, A., Kleinhenz, M. D., Scheerens, J. C., & Ling, P. P. (2007). Anthocyanin levels in nine lettuce (*Lactuca sativa*) cultivars: Influence of planting date and relations among analytic, instrumented, and visual assessments of color. *HortScience*, *42*, 232–238. https://doi.org/10.21273/HORTSCI.42.2.232

Godfray, H. C. J., Beddington, J. R., Crute, I. R., Haddad, L., Lawrence, D., Muir, J. F., … Toulmin, C. (2010). Food security: The challenge of feeding 9 billion people. *Science*, *327*, 812–818. https://doi.org/10.1126/science.1185383

Grossman, Y. L., Ustin, S. L., Jacquemond, S., Sanderson, E. W., Schmuck, G., & Verdebout, J. (1996). Critique of stepwise multiple linear regression for the extraction of leaf biochemistry information from leaf reflectance data. *Remote Sensing of Environment*, *56*, 182–193. https://doi.org/10.1016/0034-4257(95)00235-9

Guidi, L., Remorini, D., Cotrozzi, L., Giordani, T., Lorenzini, G., Massai, R., … Landi, M. (2017). The harsh life of an urban tree: The effect of a single pulse of ozone in salt-stressed *Quercus ilex* saplings. *Tree Physiology*, *37*, 246–260.

Hollman, P. C. H. (2001). Evidence for health benefits of plant phenols: Local or systemic effects? *Journal of the Science of Food and Agriculture*, *81*, 842–852. https://doi.org/10.1002/jsfa.900

Itoh, H., Nomura, K., Shiraishi, N., Uno, Y., Kuroki, S., & Ayata, K. (2015). Continuous measurement of nitrate concentration in whole lettuce plant by visible-near-infrared spectroscopy. *Environmental Control in Biology*, *53*, 205–215. https://doi.org/10.2525/ecb.53.205

Johkan, M., Shoji, K., Goto, F., Hahida, S., & Yoshihara, T. (2012). Effect of green light wavelength and intensity on photomorphogenesis and photosynthesis in *Lactuca sativa*. *Environmental and Experimental Botany*, *75*, 128–133.

Kim, H.-J., Fonseca, J. M., Choi, J.-H., Kubota, C., & Kwon, D. Y. (2008). Salt in irrigation water affects the nutritional and visual properties of romaine lettuce (*Lactuca sativa* L.). *Journal of Agriculture and Food Chemistry*, *56*, 3772–3776.

Kokaly, R. F., & Skidmore, A. K. (2015). Plant phenolics and absorption features in the vegetation reflectance spectra near 1.66 μm.

International Journal of Applied Earth Observation and Geoinformation, *43*, 55–83.

Kuhn, M. (2008). Building predictive models in R using the caret package. *Journal of Statistical Software*, *28*, 5.

Landi, M., Cotrozzi, L., Pellegrini, E., Remorini, D., Tonelli, M., Trivellini, A., … Lorenzini, G. (2019). When "thirsty" means "less able to activate the signalling wave triggered by a pulse of ozone:" A case of study in two Mediterranean deciduous oak species with different drought sensitivity. *Science of the Total Environment*, *657*, 379–390.

Lara, M. Á., Diezma, B., Lleó, L., Roger, J. M., Garrido, Y., Gil, M. I., & Ruiz-Altisent, M. (2016). Hyperspectral imaging to evaluate the effect of irrigation water salinity in lettuce. *Applied Sciences*, *6*, 412.

Letts, M. G., Phelan, C. A., Johnson, D. R. E., & Rood, S. B. (2008). Seasonal photosynthetic gas exchange and leaf reflectance characteristics of male and female cottonwoods in a riparian woodland. *Tree Physiology*, *28*, 1037–1048.

Li, L., Zhang, Q., & Huang, D. (2014). A review of imaging techniques for plant phenotyping. *Sensors*, *14*, 20078–20111.

Liu, C.-W., Sung, Y., Chen, B.-C., & Lai, H.-Y. (2014). Effects of nitrogen fertilizers on the growth and nitrate content of lettuce (*Lactuca sativa* L.). *International Journal of Environmental Research and Public Health*, *11*, 4427–4440.

Lopes, D. S. C., Moura, L. O., Neto, A. J. S., Ferraz, L. C. L., Carlos, L. A., & Martins, L. M. (2017). Spectral indices for non-destructive determination of lettuce pigments. *Food Analytical Methods*, *10*, 2807–2841.

Mao, H., Gao, H., Zhang, X., & Kumi, F. (2015). Nondestructive measurement of total nitrogen in lettuce by integrating spectroscopy and computer vision. *Scientia Horticulturae*, *184*, 1–7.

Merzlyak, M. N., Gitelson, A. A., Chivkunova, O. B., Solovchenko, A. E., & Pogosyan, S. I. (2003). Application of reflectance spectroscopy for analysis of higher plant pigments. *Russian Journal of Plant Physiology*, *50*, 704–710.

Mickelbart, M. V., Hasegawa, P. M., & Bailey-Serres, J. (2015). Genetic mechanisms of abiotic stress tolerance that translate to crop yield stability. *Nature Reviews Genetics*, *16*, 237–251.

Mo, C., Kim, G., Lim, J., Kim, M. S., Cho, H., & Cho, B.-W. (2015). Detection of lettuce discoloration using hyperspectral reflectance imaging. *Sensors*, *15*, 29511–29534.

Moura, L. O., Lopes, D. C., Neto, A. J. S., Ferraz, L. L., Carlos, L. A., & Martins, L. M. (2016). Evaluation of techniques for automatic classification of lettuce based on spectral reflectance. *Food Analytical Methods*, *9*, 1799–1806.

Mutanga, O., & Skidmore, A. K. (2007). Red edge shift and biochemical content in grass canopies. *ISPRS Journal of Photogrammetry and Remote Sensing*, *62*, 34–42.

Negrão, S., Schmöckel, S. M., & Tester, M. (2017). Evaluating physiological responses of plants to salinity stress. *Annals of Botany*, *119*, 1–11.

Neto, S. A. J., Moura, L. O., Lopes, D. C., Carlos, L. A., Martins, L. M., & Ferraz, L. C. (2017). Non-destructive prediction of pigment content in lettuce based on visible-NIR spectroscopy. *Journal of the Science of Food and Agriculture*, *97*, 2015–2022.

Nicolle, C., Carnat, A., Fraisse, D., Lamaison, J., Rock, E., Hervé, M., … Remesy, C. (2004). Characterisation and variation of antioxidant micronutrients in lettuce (*Lactuca sativa* folium). *Journal of the Science of Food and Agriculture*, *84*, 2061–2069.

Pandey, P., Irulappan, V., Bagavathiannan, M. V., & Senthil-Kumar, M. (2017). Impact of combined abiotic and biotic stresses on plant growth and avenues for crop improvement by exploiting physio-morphological traits. *Frontiers in Plant Science*, *8*, 537.

Pellegrini, E., Hoshika, Y., Dusart, N., Cotrozzi, L., Gérard, J., Nali, C., … Paoletti, E. (2019). Antioxidative responses of three oak species under ozone and water stress conditions. *Science of the Total Environment*, *647*, 390–399.

Pérez-López, U., Miranda-Apodaca, J., Lacuestra, M., Mena-Petite, A., & Munõz-Rueda, A. (2015). Growth and nutritional quality improvement in two differently pigmented lettuce cultivars grown under elevated CO_2 and/or salinity. *Scientia Horticulturae*, *195*, 56–66.

Pérez-López, U., Miranda-Apodaca, J., Munõz-Rueda, A., & Mena-Petite, A. (2013). Lettuce production and antioxidant capacity are differentially modified by salt stress and light intensity under ambient and elevated CO_2. *Journal of Plant Physiology*, *170*, 1517–1525.

Petisco, C., García-Criado, B., Mediavilla, S., Vázquez de Aldana, B. R., Zabalgogeazcoa, I., & García-Ciudad, A. (2006). Near-infrared reflectance spectroscopy as a fast and non-destructive tool to predict foliar organic constituents of several woody species. *Analytical and Bioanalytical Chemistry*, *386*, 1823–1833.

Podda, A., Pisuttu, C., Hoshika, Y., Pellegrini, E., Carrari, E., Lorenzini, G., … Paoletti, E. (2019). Can nutrient fertilization mitigate the effects of ozone exposure on an ozone-sensitive poplar clone? *Science of the Total Environment*, *657*, 340–350.

Ramirez, J. A., Posada, J. M., Handa, I. T., Hoch, G., Vohland, M., Messier, C., & Reu, B. (2015). Near-infrared spectroscopy (NIRS) predicts non-structural carbohydrate concentrations in different tissue types of a broad range of tree species. *Methods in Ecology and Evolution*, *6*, 1018–1025.

Reyes-Cin-Wo, S., Wang, Z., Yang, X., Kozik, A., Arikit, S., Song, C., … Xia, R. (2017). Genome assembly with in vitro proximity ligation data and whole-genome triplication in lettuce. *Nature Communications*, *8*, 14953.

Romero-Aranda, R., Soria, T., & Cuartero, J. (2001). Tomato plant-water uptake and plant-water relationships under saline growth conditions. *Plant Science*, *160*, 265–727.

Rubert-Nason, K. F., Holeski, L. M., Couture, J. J., Gusse, A., Undersander, D. J., & Lindroth, R. L. (2013). Rapid phytochemical analysis of birch (*Betula*) and poplar (*Populus*) foliage by near-infrared reflectance spectroscopy. *Analytical and Bioanalytical Chemistry*, *405*, 1333–1344.

Saito, Y., Shimizu, H., Nakashima, H., Miyasaka, J., & Ohdoi, K. (2010). The effect of light quality on growth of lettuce. *IFAC Proceedings Volumes*, *43*, 294-298.

Samoulienė, G., Sirtautas, R., Brazaitytė, A., & Duchovskis, P. (2012). LED lighting and seasonality effects antioxidant properties of baby leaf lettuce. *Food Chemistry*, *134*, 1494–1499. https://doi.org/10.1016/j.foodchem.2012.03.061

Schulz, H., Engelhardt, U. H., Wegent, A., Drews, H. H., & Lapczynski, S. (1999). Application of near-infrared reflectance spectroscopy to the simultaneous prediction of alkaloids and phenolic substances in green tea leaves. *Journal of Agricultural and Food Chemistry*, *47*, 5064–5067. https://doi.org/10.1021/jf9813743

Serbin, S. P. (2012). *Spectroscopic determination of leaf nutritional, morphological, and metabolic traits*. PhD thesis, University of Wisconsin–Madison, Madison, WI.

Serbin, S. P., Dillaway, D. N., Kruger, E. L., & Townsend, P. A. (2012). Leaf optical properties reflect variation in photosynthetic metabolism and its sensitivity to temperature. *Journal of Experimental Botany*, *63*, 489–502. https://doi.org/10.1093/jxb/err294

Serbin, S. P., Singh, A., Desai, A. R., Dubois, S. G., Jablosnki, A. D., Kingdon, C. C., … Townsend, P. A. (2015). Remotely estimating photosynthetic capacity, and its response to temperature, in vegetation canopies using imaging spectroscopy. *Remote Sensing of Environment*, *167*, 78–87.

Sgherri, C., Pérez-López, U., Micaelli, F., Miranda-Apodaca, J., Mena-Petite, A., Muñoz-Rueda, A., & Quartacci, M. F. (2017). Elevated CO_2 and salinity are responsible for phenolics-enrichment in two differently pigmented lettuces. *Plant Physiology and Biochemistry*, *115*, 269–278. https://doi.org/10.1016/j.plaphy.2017.04.006

Shetty, N., & Gislum, R. (2011). Quantification of fructan concentration in grasses using NIR spectroscopy and PLSR. *Field Crops Research*, *120*, 31–37. https://doi.org/10.1016/j.fcr.2010.08.008

Silvia-Perez, V., Molero, G., Serbin, S. P., Condon, A. G., Reynolds, M. P., Furbank, R. T., & Evans, J. R. (2017). Hyperspectral reflectance as a tool to measure biochemical and physiological traits in wheat. *Journal of Experimental Botany*, *69*, 483–496. https://doi.org/10.1093/jxb/erx421

Slaughter, D., Giles, K., Fennimore, S. A., & Smith, R. F. (2008). Multispectral machine vision identification of lettuce and weed seedlings for automated weed control. *Weed Technology*, *22*, 378–384. https://doi.org/10.1614/WT-07-104.1

Smith, K. L., Steven, M. D., & Colls, J. J. (2004). Use of hyperspectral derivative ratios in red-edge region to identify plant stress response to gas leaks. *Remote Sensing of Environment*, *92*, 207–217.

Sun, J., Jin, X., Mao, H., Wu, X., Gao, H., Zhu, W., & Liu, X. (2013). Detecting nitrogen content in lettuce leaves based on hyperspectral imaging and multiple regression analysis. *Information Technology Journal*, *12*, 4845–4851.

Sun, J., Ye, M., Peng, S., & Li, Y. (2016). Nitrogen can improve the rapid response of photosynthesis to changing irradiance in rice (*Oryza sativa* L.) plants. *Scientific Reports*, *6*, 31305.

Uddling, J., Gelang-Alfredsson, J., Piikki, K., & Pleijel, H. (2007). Evaluating the relationship between leaf clorophyll concentration and SPAD-502 chlorophyll meter readings. *Photosynthesis Research*, *91*, 37–46.

Wang, J., Lu, W., Tong, Y., & Yang, Q. (2016). Leaf morphology, photosynthetic performance, chlorophyll fluorescence, stomatal development of lettuce (*Lactuca sativa* L.) exposed to different ratios of red light to blue light. *Frontiers. Plant Science*, *7*, 250.

Wold, S., Sjöström, M., & Eriksson, L. (2001). PLS-regression: A basic tool of chemometrics. *Chemometrics and Intelligent Laboratory Systems*, *58*, 109–130.

Woodhouse, R., Heeb, M., Berry, W., Hoshizaki, T., & Wood, M. (1994). Analysis of remote reflection spectroscopy to monitor plant health. *Advances in Space Research*, *14*, 199–202.

Xu, C., & Mou, B. (2015). Evaluation of lettuce genotypes for salinity tolerance. *HortScience*, *50*, 1441–1446.

Xue, L., & Yang, L. (2009). Deriving leaf chlorophyll content on green-leafy vegetables from hyperspectral reflectance. *ISPRS Journal of Photogrammetry and Remote Sensing*, *64*, 97–106.

Yendrek, C. R., Tomaz, T., Montes, C. M., Cao, Y., Morse, A. M., Brown, P. J., … Ainsworth, E. A. (2017). High-throughput phenotyping of maize leaf physiological and biochemical traits using hyperspectral reflectance. *Plant Physiology*, *173*, 614–626.

Zarco-Tejada, P. J., Miller, J. R., Morales, A., Berjón, A., & Agüera, J. (2004). Hyperspectral indices and model simulation for chlorophyll estimation in open-canopy tree crops. *Remote Sensing of Environment*, *9*, 463–476. https://doi.org/10.1016/j.rse.2004.01.017

Zhang, L., Hoshika, Y., Carrari, E., Cotrozzi, L., Pellegrini, E., & Paoletti, E. (2018). Effects of nitrogen and phosphorus imbalance on photosynthetic traits of poplar Oxford clone under ozone pollution. *Journal of Plant Research*, *131*, 915–924. https://doi.org/10.1007/s10265-018-1071-4

SUPPORTING INFORMATION

Additional supporting information may be found online in the Supporting Information section.

How to cite this article: Cotrozzi L, Couture JJ. Hyperspectral assessment of plant responses to multi-stress environments: Prospects for managing protected agrosystems. *Plants, People, Planet*. 2020;2:244–258. https://doi.org/10.1002/ppp3.10080